Luminescence dosimetry: Does charge imbalance matter?

Autzen, M.; Murray, A.S.; Guerin, G.; Baly, L.; Ankjærgaard, C.; Bailey, M.; Jain, M.; Buylaert, J.-P.

Published in:
Radiation Measurements

Link to article, DOI:
10.1016/j.radmeas.2018.08.001

Publication date:
2018

Document Version
Publisher's PDF, also known as Version of record

Radiation Measurements 120 (2018) 26–32

Contents lists available at ScienceDirect

Radiation Measurements

journal homepage: www.elsevier.com/locate/radmeas

Luminescence dosimetry: Does charge imbalance matter?

M. Autzen[a,*], A.S. Murray[b], G. Guérin[c], L. Baly[d], C. Ankjærgaard[a], M. Bailey[a], M. Jain[a], J.-P. Buylaert[a,b]

[a] Center for Nuclear Technologies, Technical University of Denmark, DTU Risø Campus, Denmark
[b] Nordic Laboratory for Luminescence Dating, Department of Geoscience, Aarhus University, Denmark
[c] UMR 5060 CNRS-IRAMAT-CRP2A, Université Bordeaux 3, Maison de l'archéologie, 33607, Pessac Cedex, France
[d] Centro Aplicacions Tecnológicas y Desarrollo Nuclear (CEADEN), La Habana, Cuba

ARTICLE INFO

Keywords:
Geant4
Luminescence
OSL
Charge imbalance

ABSTRACT

We use both modelling and high dose experiments to investigate the effects of charge imbalance on luminescence. Charge entering and leaving irradiated 50 μm grains is modelled using Geant4 to predict the degree of charge imbalance a grain will experience when exposed to i) the $^{90}Sr/^{90}Y$ beta source of a Risø TL/OSL reader, ii) a 200 keV electron beam, and iii) the 'infinite-matrix' ^{40}K β spectrum. All simulations predict that between 1.4% and 2.9% more electrons enter a grain than leave, resulting in a net negative charge in the grain. The possible effects of this charge imbalance on luminescence production are discussed and experiments designed to test the resulting hypotheses; these involve giving very high doses (hundreds of kGy) to silt-sized quartz grains using low energy electrons (200 keV). Up to 700 kGy, we observe an increase in both luminescence output resulting from these high doses, and in sensitivity; above 700 kGy, both decrease. These observations, together with a slower luminescence decay during stimulation following higher doses, are consistent with the hypothesis of a decrease in hole population as a result of net accumulation of electrons during irradiation.

1. Introduction

Luminescence is widely used to estimate the dose absorbed during burial in natural minerals (*e.g.* quartz and feldspars) because they store separated charge (electrons and holes) for prolonged periods ($> 10^8$ years, e.g. Murray and Wintle, 1999) when exposed to ionising radiation. The total amount of stored charge can be calibrated in terms of dose, and knowing the dose rate allows the calculation of burial age, i.e. the time elapsed since the trapped charge was last reset to zero, usually by heat or light. The calibration of total trapped charge in terms of dose is usually undertaken by a comparison of the natural luminescence signal with that induced by a laboratory irradiation. It is clearly important that the luminescence response per unit dose is the same in the laboratory and in nature.

Luminescence models (e.g. Bøtter-Jensen et al., 2003; Bailey, 2001, 2004; Adamiec et al., 2004, 2006; Pagonis et al., 2007, 2008) commonly used to describe charge trapping and luminescence recombination in the dating of quartz and feldspar are all based on the assumption of charge neutrality during irradiation, i.e. all these models assume that the crystal contains an equal number of trapped electrons (n_e) and trapped holes (n_h) at any time. This assumption is taken to hold both in nature and in the laboratory. However, the assumption of charge neutrality is known not to apply in other fields. For instance, as the dose to an insulator (e.g. PMMA or samples under a Scanning Electron-Microscope (SEM)) increases, the incident electron beam has been observed to diverge due to the electric field developed as a result of build up of internal charge; this causes a decrease in range of subsequent electrons entering the insulator (e.g. Tanaka et al., 1979; McLaughlin, 1983). This problem has been observed in the SEM analysis of amorphous and crystalline quartz (Vigouroux et al., 1985; Stevens Kalceff et al., 1996) as well as in crystalline Al_2O_3 (Cazaux, 2004). A similar problem is observed in medical dosimetry when irradiating PMMA phantoms and monitoring the response with an ionisation chamber (e.g. Galbraith et al., 1984; Rawlinson et al., 1984; Mattsson and Svensson, 1984). This accumulation of charge can significantly affect the dose deposition through a block of plastic or glass and even cause breakdown trees (so-called Lichtenberg trees) if the charged block is tapped with a grounded needle or if the block is stressed mechanically (e.g. Gross, 1957, 1958; Zheng et al., 2008). Discharge of electrical insulators in the space industry is also recognised (Frederickson, 1996) and is known to have caused radiation-induced discharges in semi-conductor devices in satellites, leading to severe failures (Lam et al., 2012).

* Corresponding author.
E-mail address: maaut@dtu.dk (M. Autzen).

https://doi.org/10.1016/j.radmeas.2018.08.001
Received 5 December 2017; Received in revised form 18 July 2018; Accepted 1 August 2018
Available online 04 August 2018

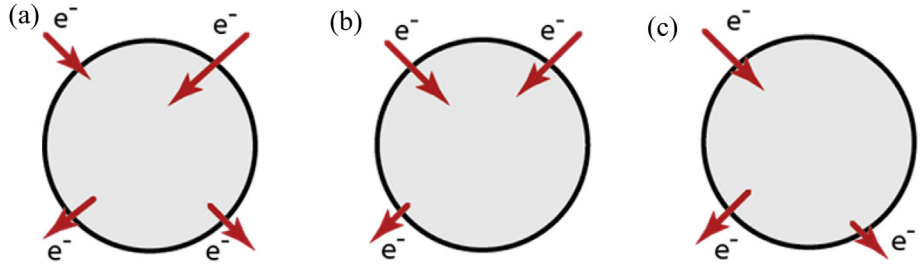

Fig. 1. a) A charge neutral grain. Each electron, which enters the grain, is balanced by an electron leaving. b) A negatively charged grain. There are more electrons entering the grain than leaving. c) A positively charged grain. There are more electrons leaving the grain than entering.

The charge state of a grain can also be changed by the emission of electrons from grain surfaces (exo-electron emission). This emission has been observed during stimulation with heat (thermally stimulated exo-electrons, TSEE) or light (optically stimulated exo-electrons, OSE) in both quartz and feldspar grains extracted from natural sediments (Ankjærgaard et al., 2006, 2008; 2009; Tsukamoto et al., 2010). The OSE signal appeared to originate from the same trap(s) as the OSL signal (same fast component characteristics) and the OSE signal strength was observed to increase with dose; these observations are evidence that a grain changes its net charge during stimulation. However, exo-electron emission will only be able to affect a fraction of the accumulated net charge; it is a surface phenomenon, involving the outer 1 nm, and thus presumably cannot affect the bulk charge.

In a matrix large compared to the range of the relevant ionising radiation (here termed an 'infinite matrix') there must be overall charge neutrality or charge conservation would be violated. However, there is no such requirement for charge neutrality on the scale of an individual grain. Thus, the number of electrons entering a grain (primary electrons) is not necessarily balanced by the number of electrons leaving the grain (primary and secondary electrons) (Fig. 1) and this charge imbalance may lead to the accumulation of net positive or negative charge in the crystal. In Fig. 1a, the grain remains neutral as the number of electrons entering and leaving the grain are the same. Even if an electron from an electron-hole pair generated inside the grain escapes it is balanced by one entering from the outside. In Fig. 1b–c, the number of electrons entering the grain is not the same as the number of electrons leaving the grain. In Fig. 1b, there will be more electrons in the grain than holes and the grain will become increasingly negatively charged. Conversely, in Fig. 1c, there will be more holes than electrons and the grain will become positively charged. In such asymmetric irradiations, the trapped hole population (n_h) will not be the same as that of the trapped electrons (n_e), i.e. the ratio $\frac{n_e}{n_h} \neq 1$. At least in principle, the limiting condition is the complete elimination of either trapped electrons or holes.

If the ratio of the number of trapped electrons to holes changes, recombination probabilities and thus luminescence are likely to be affected, either through a changed competition between recombination centres or between retrapping sites.

In this paper, we first propose a mechanism for the generation of charge imbalance and consider its possible effects on luminescence production (section 2); Geant4 modelling is then used to quantify some of these effects (section 3). Predictions from modelling are used to design an experiment to test whether charge imbalance (section 4) occurs in practice, and experimental results are presented (section 5). Finally, the implications of this model and our experimental results for accurate dosimetry are discussed.

2. Charge imbalance: mechanism and possible effect on luminescence production

When ionising radiation interacts with matter, it deposits energy in several ways, including by the generation of free electrons. On average, it takes ~4 times the band gap to generate a free electron (Wolff, 1954); the electron will then leave behind a relatively less mobile positive charge (hole). In suitable materials, these free electrons and their corresponding holes can accumulate in electron and hole traps, respectively, and in trapped charge dating the luminescence generated by these trapped charges is used to determine the absorbed dose.

In the rate equations describing luminescence production, the crystal is assumed to remain charge neutral; this implies that for every trapped electron there must also be a trapped hole. This can only be true if an equal number of electrons enters and leaves the grain. For instance, in the luminescence model developed specifically for quartz (Bailey, 2001, 2004; Adamiec et al., 2004, 2006; Pagonis et al., 2007, 2008), the rate of change in concentration of the electrons in the conduction and valence bands is determined by the ionisation rate, i.e. the number of free electron-hole pairs generated per unit energy deposited during ionisation. The ionisation rate determines both the number of electrons and of holes deposited in the crystal. This implicitly assumes charge neutrality - if all trapped electrons are released, they will recombine with all trapped holes, leaving both electron and hole traps empty.

However, it is trivial to imagine situations where this is not the case – for instance, a beta emitting grain in a non-radioactive matrix (where electrons leaving the grain are not matched by electrons entering), or irradiation of a (low-radioactivity) quartz grain by an external low-energy electron spectrum, such that most electrons entering the grain are stopped within the grain. In such circumstances, the degree to which the assumption of charge neutrality fails will depend on the size and shape of the grain as well as the energy spectrum to which the grain is exposed; the net charge remaining in or on the grain can be positive or negative.

2.1. Negative net charge

When more electrons enter the grain than leave (Fig. 1b), some of these electrons must thermalise in the interior of the grain, and so be available for trapping. Then electron traps will fill at a faster rate than hole traps. Assuming for simplicity that the electron traps are stable on the timescale of interest, the trapped electron population will eventually saturate, and electron trapping will cease. Given that in practice some electron traps are more stable than others, there will be a tendency for the excess electrons to accumulate in the deeper traps (assuming that recombination is the only way to permanently remove trapped charge). Once all electron traps are saturated, any additional extra electrons must combine with holes in either the valence band or in a hole trap, progressively reducing the net hole population without any corresponding reduction in the trapped electron population. In this scenario, the trapped hole population will eventually decrease to zero; thereafter excess (untrapped) electrons entering the grain presumably either migrate to the surface of the grain and escape, or remain in the grain, with corresponding further increase in internal stress. Reports from the gemstone industry indicate that if this process is allowed to continue, these stresses can be sufficient to crack or explode the silicate

mineral undergoing irradiation (e.g. topaz, as described in Nassau, 1985).

Qualitatively this mechanism leads to testable predictions concerning luminescence production. In low-energy electron irradiation, it is expected that, at very high doses, the trapped hole population would decrease, leading to fewer recombination sites. During subsequent optical stimulation, this would in turn lead to a decrease in the recombination rate with dose, and an increase in the rate of electron retrapping. The reduction in recombination rate would lead to a decrease of both absolute luminescence output and probably also of the subsequent luminescence sensitivity. The increase in retrapping rate would result in a corresponding slower decay of the OSL curve with stimulation time when comparing the shapes before and after a large dose.

2.2. Positive net charge

In the case of internal radioactivity, each β^- decay with sufficient electron energy to leave the grain will leave behind a positively charged atom due to charge conservation. The mean ^{40}K beta energy is 0.51 MeV, corresponding to a range of ~800 μm in quartz; thus, most electrons generated by ^{40}K decay will leave a sand-sized grain. For widely separated (i.e. low concentration) K-feldspar grains contained in a low activity matrix (*e.g.* quartz sand), where the internal ^{40}K beta decay dominates the feldspar grain dose rate, there will only be a very small flux of scattered electrons entering the grain. Then the flux of electrons leaving the grain will not be balanced by electrons entering the grain, resulting in a net positively charged ($n_e < n_h$) grain.

The accumulation of excess holes will eventually saturate all hole traps, and lead to a concentration of holes in the valence band. These may then recombine directly with trapped electrons (normally an extremely low probability event) decreasing the absolute luminescence intensity as the trapped electron population decreases. However, in contrast to the situation with an excess of electrons, an excess of holes could lead to either increased or decreased luminescence sensitivity, as measured after stimulation of the electrons remaining after the acquisition of a very large dose. The number of trapped holes available for recombination with the electrons from a test dose would be very large, but the probability of a recombination leading to photon production would depend on the ratio at saturation of the luminescent and non-luminescent hole populations.

In the case of electron irradiation, it is possible to imagine mechanisms by which charge may leak from the conduction band to the grain surface, and so to the surrounding environment; this requires that the electron has at least enough energy to overcome the electron affinity (approx. 1 eV). Such processes must take a significant period of time (otherwise the observations of beam deflection and gemstone fragmentation discussed above would not be possible), and it seems reasonable that electrons could be trapped in this time. In this article, we are concerned with the behaviour of electrons after they have been trapped.

In the following sections, we test the qualitative predictions made above under the conditions of net negative charge, using a radiation transport model (Geant4) to quantify the electron population predictions. These predictions are then compared with the result of experiments.

3. Radiation transport modelling

3.1. Modelling setup

To simulate dose rates in nature and charge imbalance in individual grains, we use Geant4 (Agostinelli et al., 2003; Allison et al., 2006). This has previously been used to model dose rates to sand-sized grains in nature (Guérin, 2011; Guérin et al., 2012, 2015) and in the laboratory (Greilich et al., 2008; Autzen et al., 2017) as well as to model electron-hole pair generation (Kovalev, 2015). Here, we use the Penelope physics model for electromagnetic interactions and a 40 eV production and tracking cut-off (corresponding to a range of $< \ < 1$ μm in quartz); at this energy the particle is considered stopped and its energy is deposited locally. It is recognised that even this cut-off is well above the 1 eV electron affinity of quartz, suggesting that, at least in principle, an electron with the cut-off energy would still have enough energy to escape from the conduction band to the grain surface. However, the range of even a 10 keV electron in quartz is ~1 μm; such electrons would be unable to reach the grain surface from more than 88% of the volume of a 50 μm diameter grain; given the very much shorter range of an electron reaching the cut-off energy of 40 eV, we presume that effectively all such electrons would thermalise to the bottom of the conduction band and be unable to reach the grain surface.

During these simulations, for every 100,000 particles emitted by the source, we record.

(i) the energy deposited in the grain
(ii) the number of electrons entering the grain
(iii) the number of electrons leaving the grain
(iv) the number of electrons generated inside the grain by ionisation.

(i) is needed to determine the dose and dose rate that the grain experiences under different conditions; we use these values to compare our simulation results with published infinite matrix dose rates (Guérin et al., 2012) and measured laboratory dose rates. The difference between (ii) and (iii) gives the net charge in the grain. The number of electron-hole pairs generated (iv) can be compared with the ionisation rate used by Bailey (2001, 2004) and Pagonis et al. (2007, 2008). See Fig. 2 for additional information on the individual irradiation geometries.

Modelling the response of a 50 μm diameter spherical quartz grain with no internal radioactivity was undertaken for several geometries: (i) in a quartz matrix (emitters: ^{40}K, see Fig. 2a), (ii) quartz grains mounted on a stainless-steel disc or in an aluminium single grain disc irradiated by a ^{90}Sr/^{90}Y beta source (Fig. 2b–c, respectively), and (iii) quartz grains on a stainless-steel disc irradiated by an electron beam (Fig. 2d). Each of the simulation geometries is described in detail in the Supplementary Material.

3.2. Modelling results and discussion

The results are presented in Table 1. The ratio of dose rates in Table 1 show that the relevant simulated dose rates are all very similar (Table 1, row 1) to those from direct calibration of the reader and those from infinite matrix dose rates (Guérin et al., 2012). The electron-hole pair generation rates per Gy (Table 1, row 2) are also very similar for the different irradiation geometries. However, the most interesting result of the modelling is that, in all geometries, more electrons enter the grain than leave (Table 1, row 3) i.e. the ratio $\frac{n_e}{n_h} > 1$ and so the grain acquires a net negative charge. While the extra electrons only contribute between 1.4 and 2.9% of the total number of electrons deposited per Gy, these electrons have no corresponding holes and thus presumably accumulate with dose/time.

Using trap concentrations from Bailey (2004), it is estimated that it will require ~130 kGy to fill all of the electron traps and ~5 MGy to recombine and so eliminate all the trapped holes. We would thus expect the population of trapped electrons to initially increase with dose and subsequently saturate when all the traps have been filled. The presence of extra electrons means that the hole population will always be a few % smaller than the electron population. Once the electron traps have all been filled, the trapped hole population should then decrease linearly as extra electrons continue to be added to the grain. This model prediction is illustrated in Fig. 3. In practice, other effects, such as charge repulsion, presumably become significant as the grain accumulates

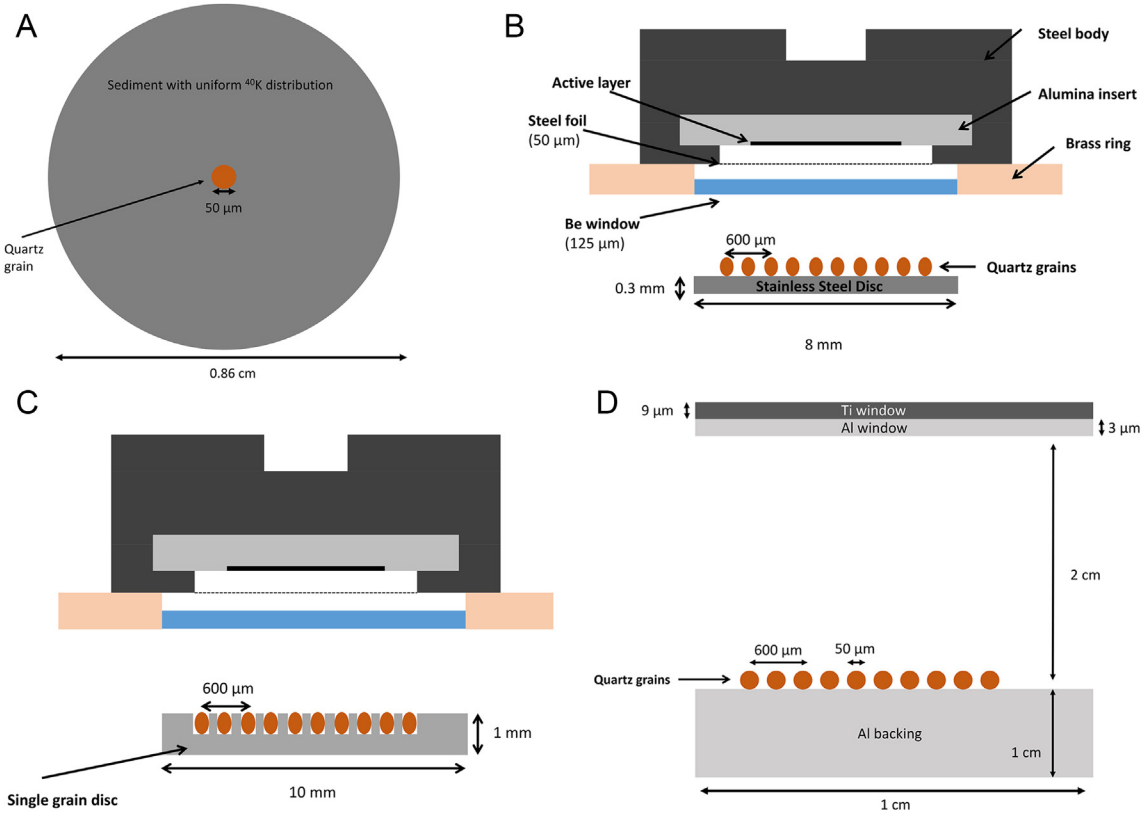

Fig. 2. a) Irradiation of a 50 µm quartz sphere sitting in sediment matrix with uniformly distributed ^{40}K emitters. b) Irradiation of 50 µm quartz spheres on a stainless steel disc in the Risø TL/OSL reader. c) Irradiation of 50 µm quartz spheres in a single grain disc. d) Irradiation of 50 µm quartz spheres in the electron beam.

more and more net negative charge, and so the prediction of a linear decrease is likely to be simplistic.

Accumulated doses of this order can be achieved over geological timescales. For example, in a granite with a dose rate of 5 Gy ka^{-1} it would take 2.6 × 10^7 years and 10^9 years to give 130 kGy and 5 MGy to a quartz grain, respectively. Doses of several tens to hundreds of kGy are not practical using our beta or gamma sources but they can be achieved using an electron beam. The model comparison between a 1.48 GBq beta source and a 200 keV electron beam is shown in Table 1. The total number of electron-hole pairs generated per unit dose delivered by the electron beam is similar to that calculated for the beta source, but because the range of the electrons in quartz (80 µm) is comparable with the grain size (50 µm) the extra electrons (net charge) make up a larger fraction of the total.

In the next sections the model prediction shown in Fig. 3 is tested experimentally.

4. Materials and methods

4.1. Instrumentation

Irradiations were carried out using:

- Risø TL/OSL DA-20 readers each fitted with a ^{90}Sr/^{90}Y beta source ($\overline{E} = 523\ keV$) of activity either 1.48 GBq or 3 GBq. Prior to irradiation, grains were mounted as a mono-layer on 0.1 mm thick stainless-steel discs using silicone oil.
- A Comet EBLab-200 electron beam. Mono-energetic 200 keV electrons (range ~ 80 µm in quartz) are emitted from a hot wire through titanium and aluminium windows to give very large dose rates at the sample position; here we have used 50 kGy s^{-1}. The stainless-steel discs containing the grains were placed on a tray which moved through the electron beam under a constant air flow to minimise temperature increase.

The dose rate delivered by the electron beam is ~10^4 times larger than that of the normal ^{90}Sr/^{90}Y beta source, and so dose rate effects

Table 1
Predictions of GEANT4 modelling of irradiations.

	TL/OSL Reader Source: 1.48 GBq ^{90}Sr/^{90}Y		^{40}K 600 Bq/kg	Electron Beam
	Stainless Steel disc	Single Grain disc	Sediment	200 keV
Ratio of dose rates (Model to Experiment)	1.03 ± 0.03[a]	0.971 ± 0.009[a]	1.02 ± 0.02[b]	
Electron/Hole pairs generated [Gy^{-1}]	(81.1 ± 0.5) × 10^3	(81.3 ± 0.4) × 10^3	(82.3 ± 1.2) × 10^3	(84.0 ± 1.3) × 10^3
Excess electrons [Gy^{-1}]	**(2.37 ± 0.05) × 10^3**	**(1.53 ± 0.04) × 10^3**	**(2.16 ± 0.13) × 10^3**	**(2.53 ± 0.11) × 10^3**
Fraction of total electrons [Gy^{-1}]	**2.49 ± 0.17%**	**1.41 ± 0.16%**	**2.63 ± 0.14%**	**2.93 ± 0.14%**

Note: a)Ratio to calibrated dose rate using calibration quartz (Hansen et al., 2015) b)Ratio to simulated dose rates in Guérin et al. (2012).

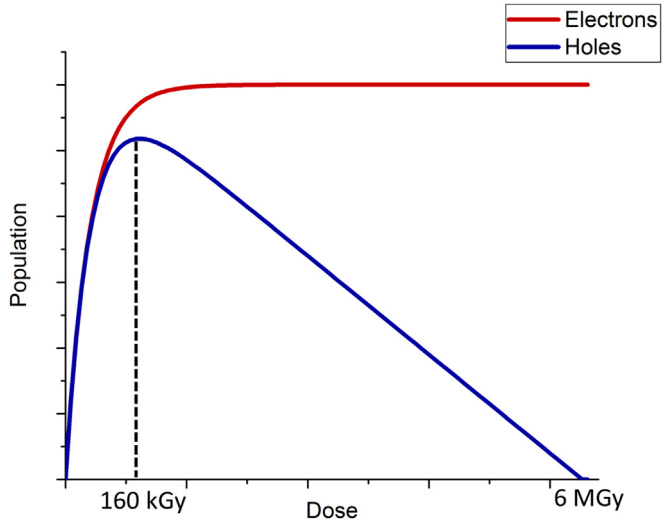

Fig. 3. Model prediction of the trapped electron population (red curve) and hole population (blue curve) in quartz when considering charge imbalance with excess electrons. (For interpretation of the references to colour in this figure legend, the reader is referred to the Web version of this article.)

(Chen and Leung, 2001) may play role in the luminescence response. On the other hand, the beta source dose rate is $\sim 10^{10}$ times larger than typical natural dose rates and yet it is still possible to measure ages to within at least 10% accuracy using OSL signals. It thus seems reasonable to assume that dose rate effects in comparing a beta source irradiation with electron beam irradiation are unlikely to be large.

4.2. Samples

Quartz extracts from two loess deposits were used to test model predictions; (i) a Chinese loess sample (sample H28112) from Stevens et al. (2016) and (ii) a composite sample of different portions of Serbian loess from a site on the Titel Loess Plateau (Marković et al., 2015). Based on initial modelling of the electron beam, a target grain size of 50 μm was chosen because this allows full penetration of the grain by 200 keV electrons while still stopping a majority of lower energy electrons. Extracts were sieved to 40–63 μm before treatment with hydrochloric acid (HCl, 10%), hydrogen peroxide (H_2O_2, conc.) to remove any carbonates and organic matter and etching with 40% HF to remove any feldspars. Finally, the samples were sieved again to > 40 μm to ensure a controlled grain size fraction.

The Chinese loess sample was pre split into two batches of which one was sensitised as described in Hansen et al. (2015), resulting in three samples for the experiment, namely Chinese loess, sensitised Chinese loess and Serbian loess. A total of 120 aliquots of each sample were prepared and the stability of the sample sensitivity after several L_x/T_x cycles was checked using the SAR protocol listed in Table 2a. The stabilised OSL sensitivity (T_x) of each aliquot to a beta test dose of 3 Gy was measured before electron beam irradiation.

Aliquots were arranged in 10 groups of 12 aliquots per sample. Each group was split equally between two aluminium trays, one sitting on a Perspex backing to preventing electrical grounding and another sitting on top of an aluminium backing and so connected to earth. The aliquots were each given a dose of 100 kGy per irradiation and 24 aliquots of each sample (12 per substrate) were removed after cumulative doses of 100 kGy, 300 kGy, 700 kGy, 1.9 MGy, and 5 MGy. Note that all of these doses are presumed to be sufficient to completely saturate the OSL trap (s). The aliquots were stored in the dark at −18 °C until all irradiations were complete.

The OSL measurements following the electron beam irradiation (Table 2b) were carried out on the same TL/OSL DA-20 readers as had been used prior to the electron beam to avoid introduction of extra uncertainties. To ensure that as much of the signal as possible was recorded and there were no more exponentially decaying components, the response to the electron beam (OSL_1 and OSL_2) was stimulated for 100 s. For all OSL records the channel width was kept constant. OSL signals were integrated from 1 to 98 s minus a background of 98–100 s (response to electron beam, OSL_1 and OSL_2) and 1–38 s minus a background of 38–40 s (response to beta test dose, OSL_3).

Table 2
Luminescence measurement sequences.

Table 2a: Luminescence measurement sequence prior to e-beam irradiation

Step	Treatment	Observation
1	Dose, 6 Gy	
2	Preheat: 260 °C for 10s	
3	OSL at 125 °C, 40 s	L_x
4	Test dose, 3 Gy	
5	TL to 220 °C	
6	OSL at 125 °C, 40 s	T_x
7	OSL at 280 °C, 40 s	
8	Return to 1	

Table 2b: Luminescence measurement sequence after to e-beam irradiation

Step	Treatment	Observation
1	TL to 150 °C	
2	OSL at 125 °C, 100 s	OSL_1
3	TL to 150 °C	
4	OSL at 125 °C, 100 s	OSL_2
5	Test dose, 3 Gy	
6	TL to 150° or 220 °C	
7	OSL at 125 °C, 40 s	OSL_3

5. Experimental results

No difference could be detected between results obtained using the aluminium and Perspex substrates during electron beam irradiations and so the results have been combined (see Fig. S2 for a comparison of signals from irradiations on Al and Perspex). The results are summarised in Fig. 4a, where the net OSL counts (OSL_1 in Table 2) are shown, averaged over all 24 aliquots at each dose point. The OSL signal increases for each of the three samples until a given dose of between 300 and 700 kGy, after which the signal decreases with dose. The peak in response occurs at a slightly lower dose (~300 kGy) in the Serbian loess extract, whereas the response of both the natural and sensitised Chinese loess extracts peaks at ~700 kGy.

The OSL response to the electron beam irradiation was measured twice (OSL_1 and OSL_2) to ensure that the subsequent OSL_3 (response from the test dose) was unaffected by any residual from the preceding large dose (see Table 2b). Fig. 4b shows the change in test-dose response (ratio T_x to OSL_3) as a result of the electron beam irradiation and subsequent OSL measurements. The shape of this OSL sensitivity change is similar to that of the response to the electron beam irradiation.

Fig. 5a presents the normalised average OSL response to the 3 Gy beta dose for all the Serbian loess aliquots before (L_x) and after (OSL_1) being given 100 kGy (the smallest dose) in the electron beam. Fig. 5b summarises similar data, but for the aliquots given 5 MGy (the largest dose) in the electron beam. A normalised decay curve of standard calibration quartz (Hansen et al., 2015) is also shown for comparison.

In Fig. 5a, the decay rates of the response before and after the 100 kGy dose are similar for the first 0.5 s of simulation; after 0.5 s the post 100 kGy signal appears to be decay more slowly. For the 5 MGy dose, the decay rate is always slower than the pre-5 MGy signal. If the hole population has indeed decreased significantly as a result of charge imbalance within the grains at high doses, then competition between recombination and retrapping would become more important. As

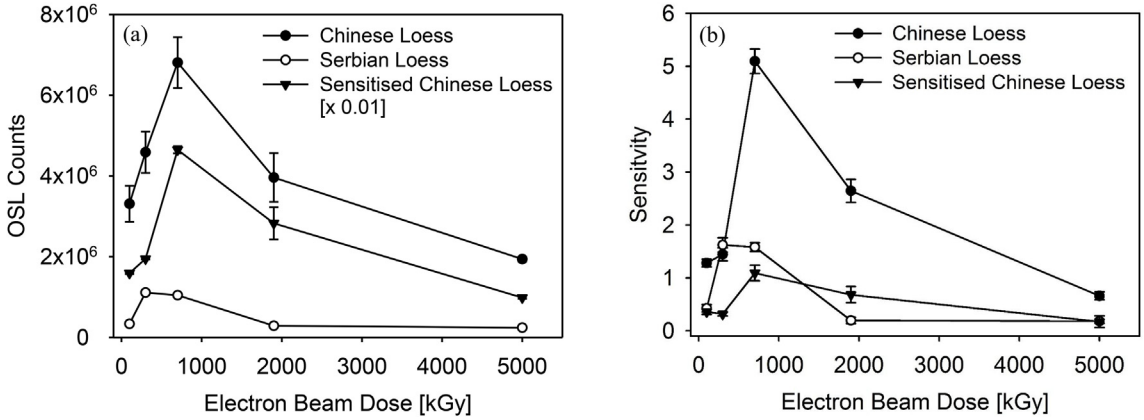

Fig. 4. a) Average background corrected total OSL signal (OSL_1) as a function of electron beam dose. b) Ratio of test dose sensitivity before and after electron beam irradiation (ratio of T_x/OSL_3) as a function of electron beam dose. Error bars represent one s.e.

retrapping probability increases, it is expected that the decay rate of the OSL stimulation curve decreases.

6. Discussion

Using modelling we have shown that during irradiation of quartz grains either in natural sediments or in the laboratory there is very likely to be a net excess of electrons entering the grain. As a result, we suggest that the net charge in the grain would become increasingly negative, and in extreme cases (very large doses, where all electron traps are saturated) the trapped hole population would begin to decrease. Fig. 3 qualitatively illustrates the expected behaviour of trapped electrons and holes separately, whereas the experimental data presented in Fig. 4 only reflect the radiative recombination probability(s). In these experiments, even the smallest electron beam irradiation (100 kGy) is presumed to saturate the OSL traps. Both Fig. 4a–b are thus interpreted as reflecting, in practice, sensitivity change, i.e. the OSL response to a constant number of electrons in the OSL trap. Fig. 4a shows the response when the OSL trap is saturated (following the large electron beam dose; presumably the number of electrons required to saturate the trap remains constant), and Fig. 4b the response when the OSL trap contains only a small (but presumably fixed) number of electrons following the test dose. In this interpretation, the change in sensitivity shown in both figures arises from a change in hole population (the OSL recombination is presumed to recombine only a small fraction of the total hole population). This initially increases towards some saturation value as the total trapped electron population increases; when the trapped electron population saturates, the hole population decreases as excess electrons resulting from the electron beam irradiations recombine with trapped holes, as predicted by the model (Fig. 3).

While competition effects between luminescent and non-luminescent centres might also contribute to the decrease in sensitivity with dose, this mechanism does not explain the significant decrease in decay rate which occurs as the dose is increased (Fig. 5a and b). This decrease is interpreted as resulting from an increase in retrapping in the electron traps, as the hole population decreases. Further measurements using exo-electron emission are planned to test this, as the exo-electron signal will not be affected by recombination pathways but only by the rate at which charge can be evicted from the conduction band.

Trap concentrations based on the model by Bailey (2004) were used to estimate the doses needed to fill all the electron traps and empty all the hole traps. From Bailey's trap concentrations and the rate at which electrons are entering the conduction band during irradiation (derived using our Geant4 modelling results) we would expect the peak in our data to be located around 130 kGy. In fact, we observe the peak between 300 and 700 kGy which is within a factor ~2–5 of what was expected from Bailey (2004) model. We consider this to be encouraging given that Bailey (2004) trap concentrations resulted from simulation optimisation and do not necessarily reflect the actual trap concentrations; these may also vary considerably between samples. Nevertheless, we do observe that the OSL sensitivity, both at saturation and at low dose, follows the shape of that expected from modelling the hole population changes with dose.

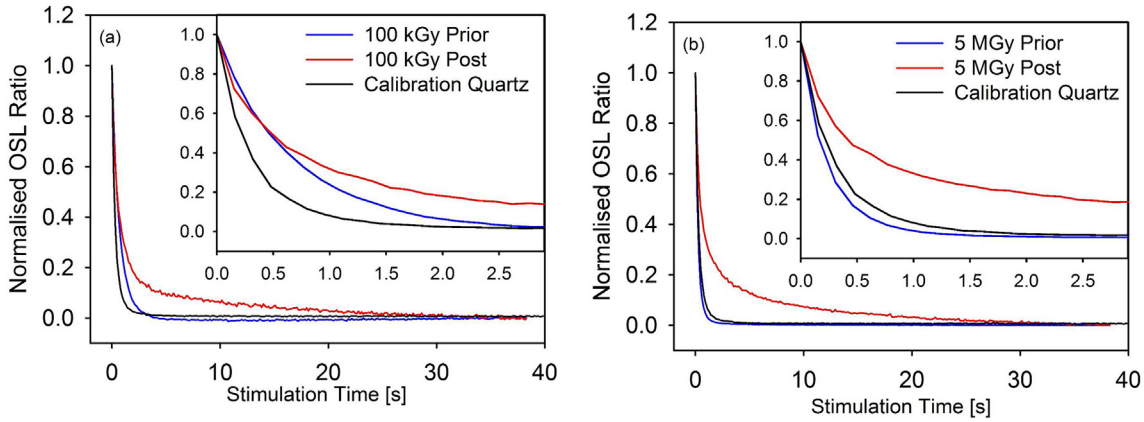

Fig. 5. a) Normalised background corrected OSL decay curve for Serbian loess for 100 kGy electron beam dose. Inset magnifies the first 2.5 s of the decay. b) Normalised background corrected OSL decay curve for Serbian loess for 5 MGy electron beam dose. Inset magnifies the first 2.5 s of the decay. Each signal is normalised to the first point. A normalised calibration quartz decay curve is shown for comparison.

We do not regard our experiments as conclusive evidence that excess electrons modify luminescence behaviour; we have not, for instance, considered the possible effects of trap creation, and dose dependent changes in ionisation rates. Nevertheless, we note that our results are broadly consistent with model predictions. In future work we will combine Geant4 results with luminescence models to quantitatively predict the impact of charge imbalance on luminescence response at small and moderate doses.

7. Conclusion

Using modelling we have demonstrated that the assumption of charge neutrality is not justified at the scale of sand-sized grains of quartz, either in nature or in the laboratory. The luminescence implications of this charge transport modelling were tested using a low energy electron beam in order to maximise any charge imbalance; the effect on luminescence production were investigated with OSL. Our data suggests that charge imbalance does exist and affects luminescence production at high doses. Although it may be possible to explain the behaviour of the luminescence response by competition between non-luminescent and luminescent centres (although this has not been shown), such an explanation does not explain the apparent slower OSL decay rates at higher doses.

Acknowledgements

M. Autzen, and J.P. Buylaert receive funding from the European Research Council (ERC) under the European Union's Horizon 2020 research and innovation programme ERC-2014-StG 639904 – RELOS. The authors would also like to thank Louise M. Helsted, Vicki Hansen, Gabor Ujvari and Warren Thompson for help in preparing samples as well as Arne Miller for lending us the electron beam.

Appendix A. Supplementary data

Supplementary data related to this article can be found at https://doi.org/10.1016/j.radmeas.2018.08.001.

References

Adamiec, G., Garcia-Talavera, M., Bailey, R.M., Iniguez de la Torre, P., 2004. Application of a genetic algorithm to finding parameter values for numerical simulations of quartz luminescence. Geochronometria 23, 9–14.
Adamiec, G., Bluszcz, A., Bailey, R., Garcia-Talavera, M., 2006. Finding model parameters: genetic algorithms and the numerical modelling of quartz luminescence. Radiat. Meas. 41, 897–902.
Agostinelli, S., Allison, J., Amako, K., Apostolakis, J., Araujo, H., Arce, P., et al., Geant4 Collaboration, 2003. Geant4 – a simulation toolkit. Nucl. Instrum. Methods Phys. Res., Sect. A 506 (3), 250–303.
Allison, J., Amako, K., Apostolakis, J., Araujo, H., Arce, P., Asai, M., et al., 2006. (Geant4 Collaboration). Geant4 development and applications. IEEE Trans. Nucl. Sci. 53 (1), 270–278.
Ankjærgaard, C., Murray, A.S., Denby, P.M., Bøtter-Jensen, L., 2006. Measurement of optically and thermally stimulated electron emission from natural minerals. Radiat. Meas. 41 (Sp. Iss.), 780–786.
Ankjærgaard, C., Denby, P.M., Murray, A.S., Jain, M., 2008. Charge movement in grains of quartz studied using exo-electron emission. Radiat. Meas. 43 (2–6), 273–277.
Ankjærgaard, C., Murray, A.S., Denby, P.M., Jain, M., 2009. Using optically stimulated electrons from quartz for the estimation of natural doses. Radiat. Meas. 44 (3), 232–238.
Autzen, M., Guérin, G., Murray, A.S., Thomsen, K.J., Buylaert, J.-P., Jain, M., 2017. The effect of backscattering on the beta dose absorbed by individual quartz grains. Radiat. Meas. 106, 491–497.
Bailey, R.M., 2001. Towards a general kinetic model for optically and thermally stimulated luminescence of quartz. Radiat. Meas. 33, 17–45.
Bailey, R.M., 2004. Paper I – simulation of dose absorption in quartz over geological timescales and its implications for the precision and accuracy of optical dating. Radiat. Meas. 38, 299–310.
Bøtter-Jensen, L., McKeever, S.W.S., Wintle, A.G., 2003. Optically Stimulated Luminescence Dosimetry. Elsevier, Amsterdam (Chapter 2).
Cazaux, J., 2004. Scenario for time evolution of insulator charging under various focused electron irradiations. J. Appl. Phys. 95, 731.
Chen, R., Leung, P.L., 2001. Nonlinear dose dependence and dose-rate dependence of optically stimulated luminescence and thermoluminescence. Radiat. Meas. 33, 475–481.
Frederickson, A.R., 1996. Upsets related to spacecraft charging. IEEE Trans. Nucl. Sci. 43 (2), 426–441.
Galbraith, D.M., Rawlinson, J.A., Munro, P., 1984. Dose errors due to charge storage in electron irradiated plastic phantoms. Med. Phys. 11 (2), 197–203.
Greilich, S., Murray, A.S., Bøtter-Jensen, L., 2008. Simulation electron transport during beta irradiation. Radiat. Meas. 43 (2–6), 748–751.
Gross, B., 1957. Irradiation effects in borosilicate glass. Phys. Rev. 107 (2), 368–373.
Gross, B., 1958. Irradiation effects in plexiglas. J. Polym. Sci. 27, 135–143.
Guérin, G., 2011. Modélisation et simulation des effects dosimétriques dans les sédiment quaternaires : application aux méthodes de datation par luminescence. PhD thesis. Université Bordeaux.
Guérin, G., Mercier, N., Nathan, R., Adamiec, G., Lefrais, Y., 2012. On the use of the infinite matrix assumption and associated concepts: a critical review. Radiat. Meas. 47 (9), 778–785.
Guérin, G., Jain, M., Thomsen, K.J., Murray, A.S., Mercier, N., 2015. Modelling dose rate to single grains of quartz in well-sorted sand samples: the dispersion arising from the presence of potassium feldspars and implications for single grain OSL dating. Quat. Geochronol. 27, 52–65.
Hansen, V., Murray, A., Buylaert, J.P., Yeo, E.Y., Thomsen, K., 2015. A new irradiated quartz for beta source calibration. Radiat. Meas. 81, 123–127.
Kovalev, I.V., 2015. Electron-hole pairs generation rate estimation irradiated by isotope Nickel-63 in silicone using Geant4. IOP Conf. Ser. Mater. Sci. Eng. 94, 012024.
Lam, H.-L., Boteler, D.H., Burlton, B., Evans, J., 2012. Anik-E1 and E2 satellite failures of January 1994 revisited. Space Weather 10 S1003.
Marković, S.B., Stevens, T., Kukla, G.J., Hambach, U., Fitzsimmons, K.E., Gibbard, P., Buggle, B., Zech, M., Guo, Z., Qingzhen, H., Haibin, W., Dhand, O.K., Smalley, I.J., Gábor, U., Sümegi, P., Timar-Gabor, A., Veres, D., Sirocko, F., Vasiljević, D.A., Jary, Z., Svensson, A., Jović, V., Lehmkuhl, F., Kovács, J., Svirčev, Z., 2015. Danube loess stratigraphy – towards a pan-European loess stratigraphic model. Earth Sci. Rev. 148, 228–258.
Mattsson, L.O., Svensson, H., 1984. Charge build-up effects in insulating phantom materials. Acta Radiol. Oncol. 23, 393–399.
McLaughlin, W.L., 1983. Radiation processing dosimetry. Radiat. Phys. Chem. 21 (4), 359–366.
Murray, A.S., Wintle, A.G., 1999. 1999. Isothermal decay of optically stimulated luminescence in quartz. Radiat. Meas. 30, 119–125.
Nassau, K., 1985. Altering the color of topaz. Gems Gemol. 21 (No. 1), 26.
Pagonis, V., Chen, R., Wintle, A.G., 2007. Modelling thermal transfer in optically stimulated luminescence of quartz. J. Phys. Appl. Phys. 40, 998–1006.
Pagonis, V., Wintle, A.G., Chen, R., Wang, X.L., 2008. A theoretical model for a new dating protocol for quartz based on thermally transferred OSL (TT-OSL). Radiat. Meas. 43, 704–708.
Rawlinson, J.A., Bielajew, A.F., Munro, P., Galbraith, D.M., 1984. Theoretical and experimental investigation of dose enhancement due to charge storage in electron-irradiated phantoms. Med. Phys. 11 (6), 814–821.
Stevens, T., Buylaert, J.-P., Lu, H., Thiel, C., Murray, A., Frechen, M., Yi, S., Zeng, L., 2016. Mass accumulation rate and monsoon records from Xifeng, Chinese Loess Plateau, based on a luminescence age model. J. Quat. Sci. 31, 391–405.
Stevens Kalceff, M.A., Phillips, M.R., Moon, A.R., 1996. Electron irradiation-induced changes in the surface topology of silicon dioxide. J. Appl. Phys. 80, 4308.
Tanaka, R., Sunaga, H., Tamura, N., 1979. The effect of accumulated charge on depth dose profile in poly(methylmethacrylate) irradiated with fast electron beam. IEEE Trans. Nucl. Sci. NS-26 (4), 4670–4675.
Tsukamoto, S., Murray, A.S., Ankjærgaard, C., Jain, M., Lapp, T., 2010. Charge recombination processes in minerals studied using optically stimulated luminescence and time-resolved exo-electrons. J. Phys. Appl. Phys. 43 (32), 325502.
Vigouroux, J.P., Duraud, J.P., Le Moel, A., Le Gressus, C., Griscom, D.L., 1985. Electron trapping in amorphous SiO2 studied by charge buildup under electron bombardment. J. Appl. Phys. 57, 5139.
Wolff, P.A., 1954. Theory of electron multiplication in silicon and germanium. Phys. Rev. 95 (6), 1415–1420.
Zheng, F., Zhang, Y., Xiao, C., Xia, J., An, Z., 2008. Effect of applied mechanical stress on space charge breakdown in electron beam irradiated polymethyl methacrylate. IEEE Trans. Dielectr. Electr. Insul. 15 (4), 965–973.